CHAPTER IV

Determination of Orientational Order Parameter from X-ray Diffraction Measurements on Three Laterally Fluorinated Compounds

4.1. Introduction:

The order parameter in nematic liquid crystals is one of the most important physical parameters which critically affect its performance in display devices, since the anisotropies of the dielectric, optical and magnetic properties depend on the order parameter in a more or less straight forward way [1-7]. With this view in mind, the Orientational Order Parameters (OOPs) of three laterally fluorinated liquid crystalline compounds (compounds **1**, **10** and **11** mentioned in Chapter II) from x-ray diffraction and optical birefringence measurements have been determined. As discussed in Chapter II, the interesting feature of these molecules is the presence of laterally fluorinated (polar) substituents, which induces a dipole moment perpendicular to the long axes of the molecule, thereby resulting in molecules with negative dielectric anisotropy ($\Delta\varepsilon<0$) [8]. The study of the physical properties of these negative dielectric anisotropy materials has become increasingly important after the successful development of the Vertical Alignment (VA) mode technology [8-11] for Active Matrix Addressed Liquid Crystal Displays (AMLCD's). Fluorinated nematogens are also promising materials from display point of

view due to their broad nematic mesomorphic range, low rotational viscosity and high negative dielectric anisotropy ($\Delta\varepsilon < 0$) [12-14]. Moreover, the study of the birefringence (Δn) of these materials is also important so that they may be adjusted to fit the precise display configuration [15].

In this work, three laterally fluorinated compounds (compounds **1**, **10** and **11**) were investigated by x-ray diffraction and refractive index measurements. Of these, two of them have a phenyl bicyclohexane core (compounds **10** and **11**) and the third compound is a terphenyl derivative (compound **1**). Detailed x-ray diffraction measurements were done throughout the mesomorphic range of these three compounds. The Orientational Order Parameters (OOPs), $\langle P_2 \rangle$ and $\langle P_4 \rangle$, apparent molecular length or layer spacing (D in Å) and intermolecular distance (l in Å) were determined as a function of temperature. The ordinary and extraordinary refractive indices (n_o and n_e) have been determined from refractive index measurements using thin prism technique [16]. The n_o and n_e values and the density data have been used to determine the Orientational Order Parameter ($\langle P_2 \rangle$) using the standard Vuks isotropic model [17]. The $\langle P_2 \rangle$ values determined from the refractive index data have been compared with those obtained from x-ray diffraction studies. These values have also been compared with the theoretical values of Maier-Saupe [18] for the compound having only nematic phase and McMillan's theory [19-20] for compounds having both smectic and nematic phases.

4.2. Materials:

The chemical structure and transition temperatures of the compounds are shown in Table 4.1.

Table 4.1. Chemical structure and transition temperatures of compounds **1**, **10** and **11**.

*Comp. No.	Structure	T_m (°C)	T_{SmB-N} (°C)	T_{NI} (°C)
1	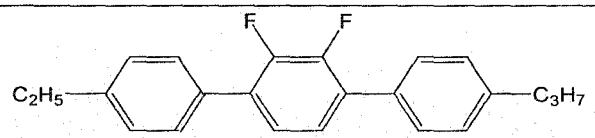	73	-----	110
10	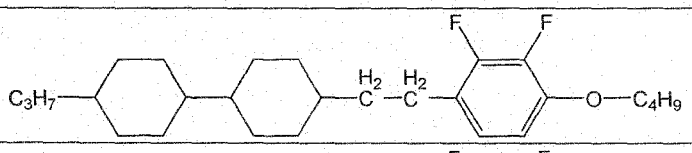	112	(110)	152
11	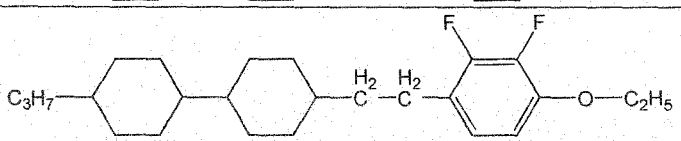	111	(109)	162

*Compound numbers are as indicated in Chapter II
(..) indicates monotropic transition.

4.3. Texture studies:

As discussed in chapter III, typical thread-like textures characteristic of the nematic phase were observed upon heating for all the compounds. Upon cooling, compound **10** and compound **11** exhibited monotropic smectic B phase with mosaic texture, while compound **1** showed only nematic phase. All the compounds showed large super cooling.

4.4. Differential Scanning Calorimetric (DSC) measurements:

The phase transition temperatures were also determined using differential scanning calorimetry (DSC) studies. The temperature variation of the heat entropy for compounds **1**, **10** and **11** are shown in Figures 4.1(a)-4.1(c).

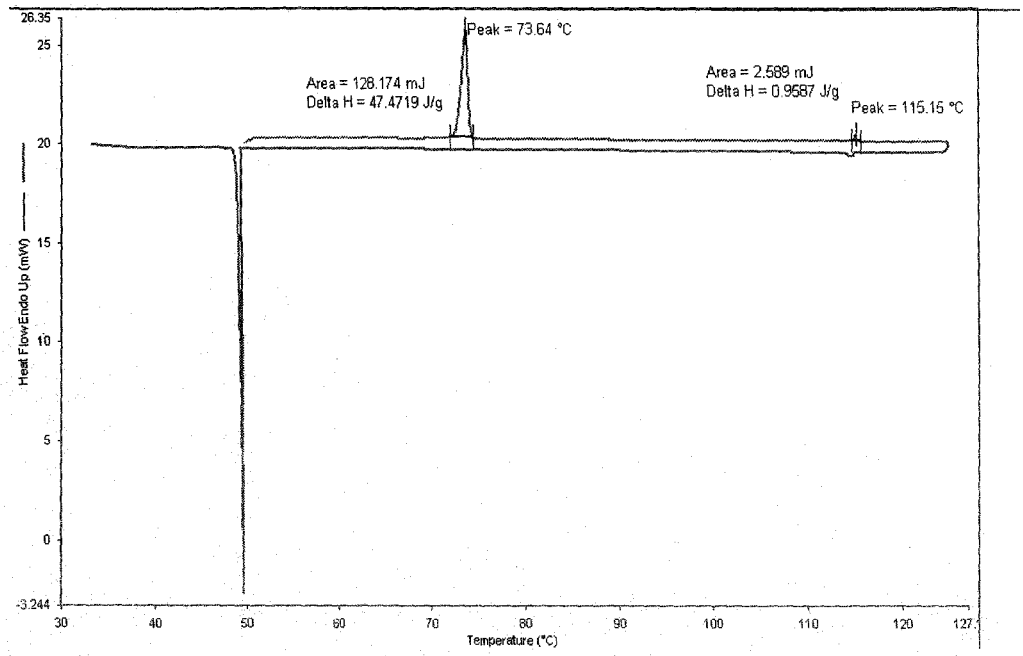

(a)

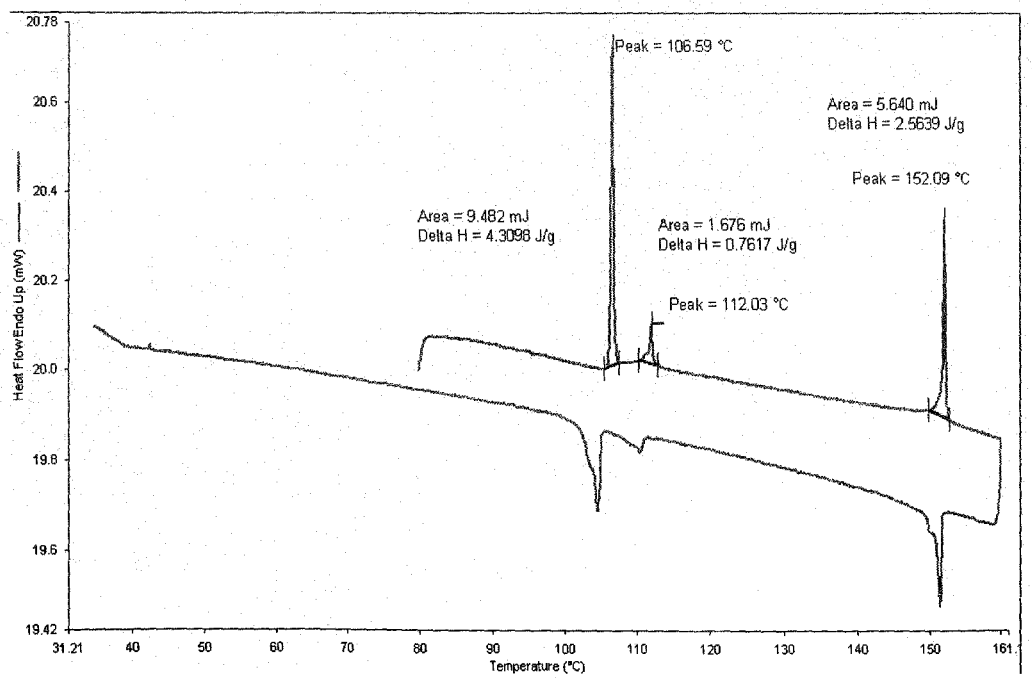

(b)

Figure 4.1. Temperature variation of heat entropy (ΔH in mW). (a) Comp. **1** and (b) Comp. **10**.

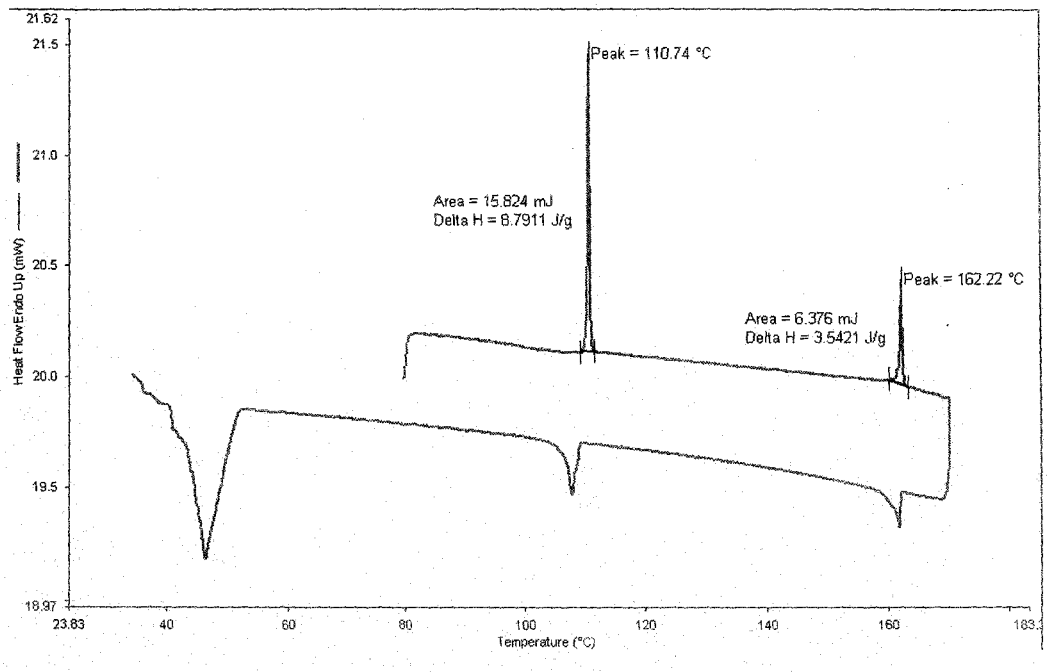

(c)

Figure 4.1. 'contd. Temperature variation of heat entropy (ΔH in mW). (c) Comp. **11**.

It is observed that the entropy change associated with the nematic - smectic B (N-Sm B) transition for compound **10** is much higher than those observed at the nematic-isotropic (N-I) transition. On the contrary, there is a smaller entropy change at the N-Sm B transition for compound **11**, in comparison to the N-I transition. Compound **1** however shows normal temperature dependence.

4.5. Density measurements:

The density of the compounds was measured by dilatometer of capillary type. The temperature variation of the density values for compounds **1**, **10-11** are shown in Figure 4.1. There is a discontinuity in the density values at the nematic - smectic B phase transition of compound **10** and compound **11**. The accuracy of density measurement is 0.1%.

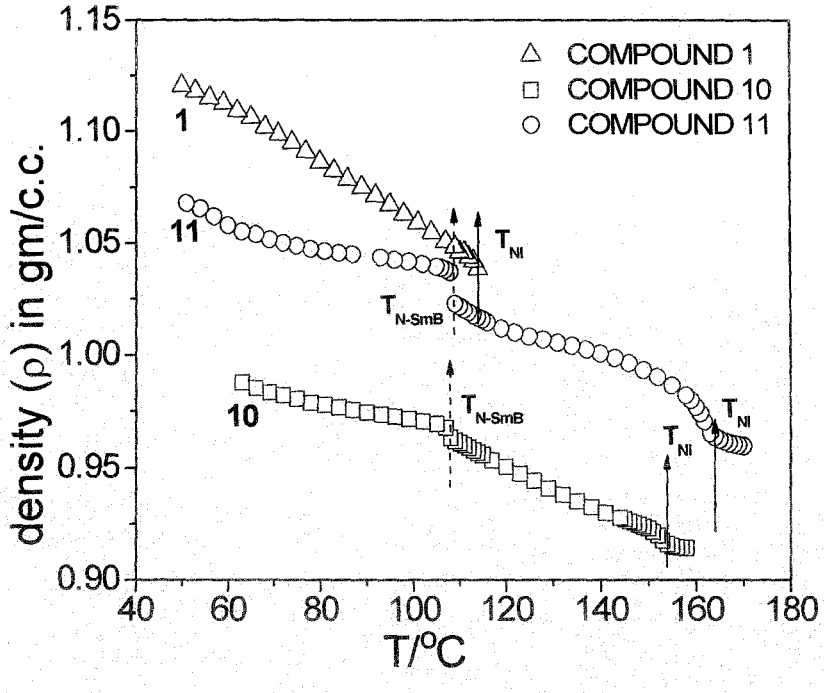

Figure 4.2. Variation of density values, ρ, as a function of temperature. Δ Comp. **1**; □ Comp. **10**; ○ Comp. **11**. T_{NI} = nematic–isotropic transition temperature; T_{SmB-N} = smectic B–nematic transition temperatures.

It has been found that the density value is highest for compound **1** (1.125gm/c.c. at around 50°C) and lowest for compound **10** (0.988gm/c.c. at around 50°C).

4.6. Refractive index measurements:

The temperature dependence of the principal refractive indices n_o and n_e and the refractive index in the isotropic phase (n_{iso}) at a wavelength of λ = 632.8 nm for the three compounds were measured (as discussed in chapter III). Similar to the density values, there is an abrupt jump in the birefringence values at the N-SmB transition for compound **10** and compound **11**. Compound **3** shows the highest birefringence of around 0.24 at 50°C. This is due to the presence of conjugated π-bond in the rigid core of the terphenyl derivative

(compound **1**). It may be mentioned that recent efforts are being made to synthesize such high birefringence materials which also combine the necessary rotational viscosity and polarity, to facilitate reduction in the cell gap for display devices [21-25].

Using the refractive indices (n_o, n_e) and the density values, the principal molecular polarizabilities (α_o, α_e) and hence the polarizability anisotropy ($\Delta\alpha$) were calculated using Vuks method [17]. The Orientational Order Parameter $<P_2>$ can be determined from the relation

$$< P_2 >= \frac{\alpha_e - \alpha_o}{\alpha_{\parallel} - \alpha_{\perp}} = \frac{\Delta\alpha}{\Delta\alpha_0} \qquad (4.1)$$

where, α_o and α_e are the effective polarizabilities for the extraordinary and ordinary rays respectively and $\alpha_{\parallel}$ and $\alpha_{\perp}$ are the polarizabilities parallel and perpendicular to the long axis of the molecule in the solid state. The polarizability anisotropies in the perfectly ordered state ($\Delta\alpha_0$) were determined from the Haller's extrapolation method [26] using the equation,

$$\Delta\alpha = \Delta\alpha_0 (1 - \frac{T}{T*})^{\beta} \qquad (4.2)$$

where $\Delta\alpha_0$, T* and β are adjustable parameters. The calculated values of $\Delta\alpha_0$, T* and β are listed in Table 4.2. It may be mentioned that for compound **10** and compound **11**, equation 4.2 have been fitted by taking the values of Δn only in the high temperature nematic phase.

Table 4.2. Values of adjustable parameters $\Delta\alpha_0$, T* and exponent β.

Compound Number	$\Delta\alpha_0 \times 10^{24}$	T* in K	β
1	16.31± 0.14	382.1± 0.2	0.20±0.003
10	7.93±0.18	425.9± 0.5	0.11±0.01
11	10.87±0.41	425.9±0.4	0.24±0.02

4.7. X-ray diffraction measurements:

X-ray diffraction patterns were recorded throughout the entire mesomorphic range for compounds **1**, **10** and **11**. X-ray diffraction photographs of compound **10** in the nematic phase (114°C) and smectic B phase (82°C) are shown in Figures 4.2(a) - (b). In the nematic phase, the outer halo is split into two crescents for each of which the intensity is maximum in the equatorial direction, whereas in the smectic B phase, this halo is replaced by sharp crescents of relatively intense diffuse scattering on both sides of the equatorial maxima. In the meridional direction, second order reflections are observed both in the nematic and smectic B phases. The angular distribution of the x-ray diffraction intensities of well oriented monodomain samples (compounds **1**, **10** and **11**) were utilized to obtain the orientational distribution function $f(\theta)$, and hence the Orientational Order Parameters (OOPs), $\langle P_2 \rangle$ and $\langle P_4 \rangle$, following a procedure reported by Bhattacharya *et. al* [27].

Figure 4.4 (a) - (c) shows the variation of the experimentally determined OOPs with temperature for all the three compounds studied. The experimental $\langle P_2 \rangle$ and $\langle P_4 \rangle$ values are found to be discontinuous across the N-Sm B phase transition for compounds **10** and **11**. Also, these values are found to be relatively high in the smectic B phase for both of these compounds, showing the phase to be much more orientationally ordered than the neighbouring nematic phase. It may be mentioned that although the approximation used for calculating $\langle P_L \rangle$ (L= 2, 4) is not valid for $\langle P_2 \rangle$ greater than 0.8, these values are still being reported, since at least qualitatively they show a degree of ordering of these fluorinated molecules possessing smectic B phase for which such values are rare [28].

The experimental data have been fitted with those calculated from McMillan's theory for smectic A [19, 20] phase for compounds **10** and compound **11** using the potential parameters α and δ as two adjustable constants, due to lack of other alternatives.

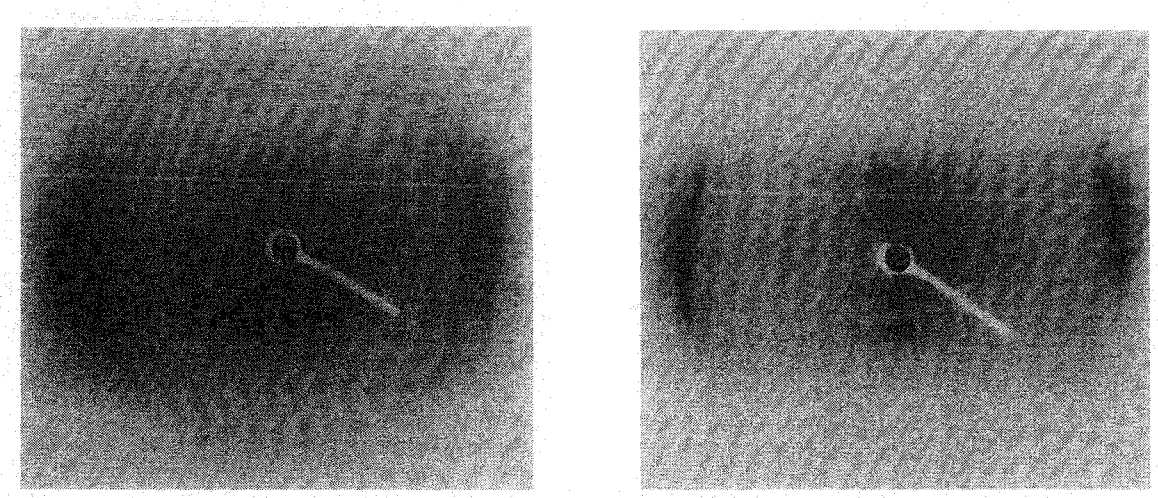

(a) (b)

Figure 4.3. X-ray diffraction photographs from aligned compound **1** in (a) nematic (114°C) and (b) smectic B (82°C) phases.

In the calculation using McMillan's model, the parameter α which varies with the chain length has been varied keeping the parameter, δ fixed (δ = 0.25). The best fitted theoretical curves were obtained for α equal to 0.55 and 0.52 for compound **10** and compound **11** respectively. The agreement between the experimental and theoretical values seems to be fair for compound **10** and fairly good for compound **11**. For compound **3,** a very good agreement is observed between the experimental $\langle P_2 \rangle$ and $\langle P_4 \rangle$ values and theoretical Maier – Saupe values. Also shown in Figures 4.4(a)-4.4(c) are the $\langle P_2 \rangle$ values determined from refractive index measurements on compounds **1**, **10** and **11**. It has been again found that there is a discontinuity in the $\langle P_2 \rangle$ values determined from refractive index data for compounds **10** and **11** near the nematic to Smectic B (N-SmB) phase transition. The Sm B liquid crystal in the vicinity of N-SmB transition is perhaps subject to an unusually short-range disorder while maintaining well-defined long range order [29].

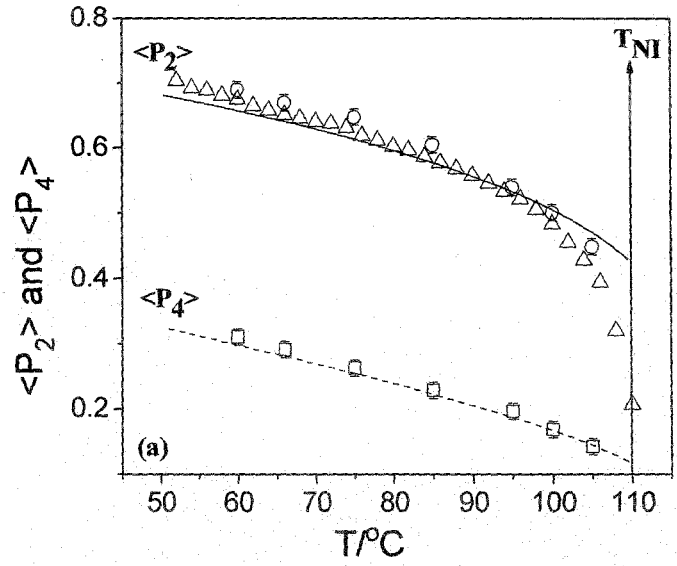

(a)

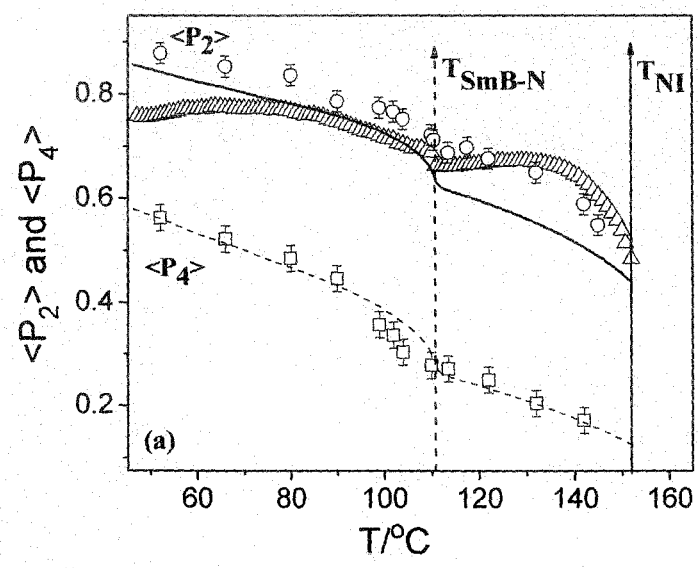

(b)

Figure 4.4. Temperature variation of Orientational Order Parameters $\langle P_2 \rangle$ and $\langle P_4 \rangle$ for (a) comp. **1** and (b) comp. **10**. ○ = x-ray data for $\langle P_2 \rangle$, □ = x-ray data for $\langle P_4 \rangle$, Δ refractive index data for $\langle P_2 \rangle$, —— $\langle P_2 \rangle$ from McMillan's theory (or Maier Saupe theory), ---- $\langle P_4 \rangle$ from McMillan's theory (or Maier- Saupe theory). T_{NI} = nematic-isotropic transition temperature. T_{SmB-N} = smectic B-nematic transition temperatures.

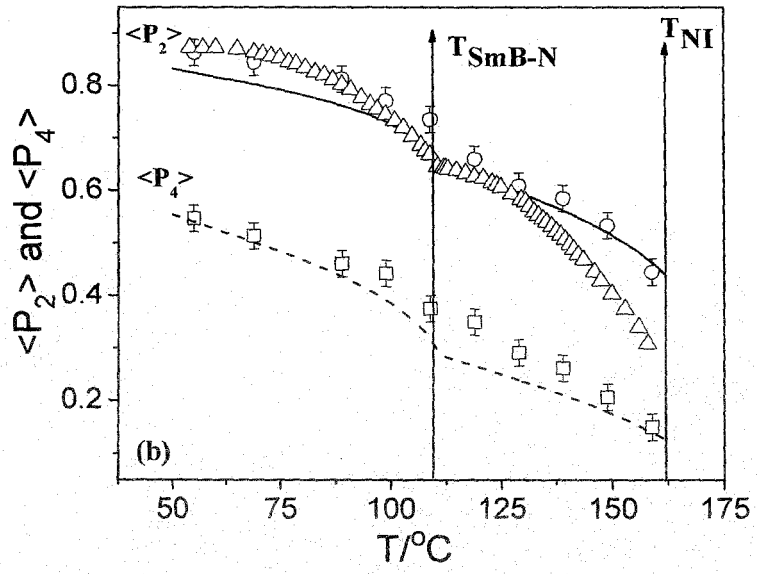

(c)

Figure 4.4. 'contd. Temperature variation of Orientational Order Parameters $\langle P_2 \rangle$ and $\langle P_4 \rangle$ for (c) Comp **11**. ○ = x-ray data for $\langle P_2 \rangle$, □ = x-ray data for $\langle P_4 \rangle$, Δ refractive index data for $\langle P_2 \rangle$, —— $\langle P_2 \rangle$ from McMillan's theory (or Maier Saupe theory), ---- $\langle P_4 \rangle$ from McMillan's theory (or Maier- Saupe theory). T_{NI} = nematic-isotropic transition temperature. T_{SmB-N} = smectic B-nematic transition temperatures.

The experimental $\langle P_2 \rangle$ values obtained from refractive index and x-ray diffraction measurement agree fairly well for compound **10** and also for compound **11**, except very near the N-I transition, in spite of the fact that two different techniques have been employed to determine the Orientational Order Parameters (OOPs) of these compounds. Lower values of the order parameter from refractive index measurement near the N-I transitions may be due to strong thermal fluctuations of the chain part of the molecules.

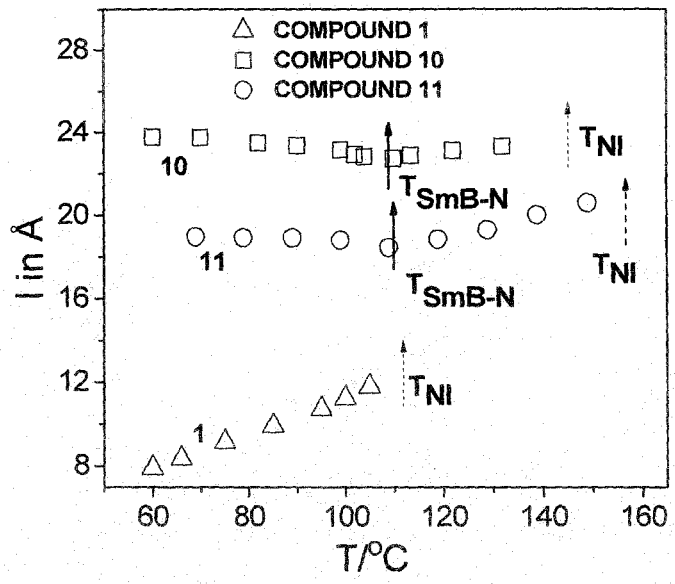

Figure 4.5. Temperature dependences of l (apparent molecular length) values for: Δ Comp **1**; □ Comp. **10** and ○ Comp. **11**.

The temperature variation of the layer spacing, D, or apparent molecular length, l, for all the compounds is shown in Figure 4.5. For both compound **10** and **11**, the values of the smectic layer spacing, d remains almost constant in the smectic B phase. In the nematic phase, the apparent molecular length, l increases slightly with increase in temperature for both **10** and **11**. This is probably due to the increased thermal vibrations of the chain parts just before the transition. It was found that the intermolecular distance (D), increases with increasing temperature, caused once again by the increasing thermal vibrations of the molecules (Figure 4.6) [28].

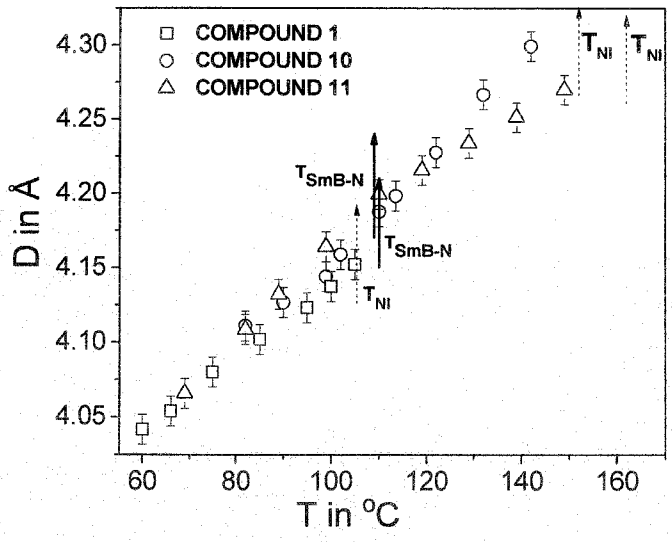

Figure 4.6. Temperature dependences of D (layer spacing) values for: □ Comp. **1**; ○ Comp. **10** and Δ Comp **11**.

4.8. Summary and Conclusions:

The physical properties of three laterally fluorinated liquid crystalline compounds **1**, **10** and **11**, have been studied by different experimental techniques. From density, refractive index and $\langle P_2 \rangle$ values determined from the x-ray diffraction and refractive index measurements, the order of the N-SmB phase transition is found to be discontinuous for both **10** and **11**. Fairly good agreement is observed between the experimental and theoretically calculated $\langle P_2 \rangle$ and $\langle P_4 \rangle$ values for **10** and **11**, even though the McMillan model is strictly valid for the smectic A phase. $\langle P_2 \rangle$ values determined from x-ray diffraction measurements are found to be in fairly good agreement with those obtained from refractive index measurements even after considering the different assumptions and approximations involved in the order parameter determination from x-ray diffraction and refractive index measurements.

References:

[1] W.H. de Jeu, *Physical Properties of Liquid Crystalline Materials.* Gordon and Breach, New York, (1980).

[2] W. Kuczyński, B. Żywuchki and J. Matecki, *Mol. Cryst. Liq. Cryst.*, ***1***, 381 (2002).

[3] (a) M.K. Das, G. Sarkar, B. Das, R. Rai and N. Sinha, *J. Phys.: Condens. Matter.*, ***24***, 115101 (2012) and (b) A. Chakraborty, B. Das, M.K. Das, S. Findeisen-Tandel, M.G. Tamba, U. Baumeister, H. Kresse and W. Weissflog, *Liq. Cryst.*, ***38(9)***, 1085 (2011).

[4] M.K. Das, A. Pramanik, B. Das, Ł Szczuciński and R Dabrowski, *J. Phys. D: Appl. Phys.*, ***45***, 415304 (2012).

[5] P.D. Roy, A. Prasad and M.K. Das, *J. Phys.: Condens. Matter.*, ***21(7)***, 075106 (2009).

[6] A. Prasad and M.K. Das, *J. Phys.: Condens. Matter.*, ***22***, 195106 (2010)

[7] P. Dasgupta, M.K. Das and B. Das, *Mol. Cryst. Liq. Cryst.*, ***540***, 154 (2011).

[8] M.F. Schiekel and K. Fahrenschon, *Appl. Phys. Lett.*, ***19***, 391 (1971).

[9] T. Sujiyama, Y. Toko, T. Hashimoto, K. Katoh, Y. Limura and S. Kobayashi, *J.Phys. D: Appl. Phys.*, ***8***, 1575 (1975).

[10] M. Schadt and W. Helfrich, *Appl. Phys. Lett.*, ***18***, 127 (1971).

[11] S.H. Hong, Y.H. Jeong, H.Y. Kim, H.M. Cho, W.G. Lee and S.H. Lee, *J. Appl. Phys.*, ***87***, 8259 (2000).

[12] S. Ghosh, P. Nayek, S. K. Roy, T.P. Majumder and R. Dabrowski, *Liq. Cryst.*, ***37***, 369 (2010).

[13] M.R. Cargilla, G. Sandforda, A.J. Tadeusiaka, G.D. Loveb, N. Hollfelderc, F. Pleisc, G. Nellesc and P. Kilickiranc, *Liq. Cryst.*, ***38***, 1069 (2010).

[14] J.W. Goodby, *Liq. Cryst.*, ***38***, 1363 (2011).

[15] D. Pauluth and K. Tarumi, *J. Mater. Chem.*, ***14***, 1219 (2004).

[16] A. Prasad and M. K. Das, *Phase Trans.*, ***83***, 1072 (2010).

[17] M. F. Vuks, *Opt. Spectros.*, ***20***, 361 (1966).

[18] W. Maier and A. Saupe, *Z. Naturforsch Tail II*, ***15a***, 287 (1960).

[19] W.L. McMillan, *Phys. Rev. A*, ***4***, 1238 (1971).

[20] W.L. McMillan, *Phys. Rev. A*, ***6***, 93 (1972).

[21] S. Gauza, P. Kula, X. Liang, S.T. Wu and R. Dabrowski , *Mol. Cryst. Liq. Cryst.*, ***509***, 47 (2009).

[22] D.S. Seo, *Liq. Cryst.*, ***27(9)***, 1147 (2000).

[23] Y. Koike, S. Kataoka, T. Sasaki, H. Chida, H. Tsuda, A. Takeda and K. Ohmuro, *AM-LCD'97 Digest*, **25** (1997).

[24] S. Shimizu, Y. Ochi, A. Nakano and M. Bone, *Soc. Info. Disp. Symp. Digest.* **72** (2004).

[25] Y.B. Kim and I.K. Hur, *J. of Inf. Disp.*, ***2(3)***, 565 (2001).

[26] (a) I. Haller, H.A. Huggins, H.R. Lilienthal and T.R. McGuire, *J. Phys. Chem.*, *77*, 950 (1973) and (b) I. Haller, *Prog. Solid State Chem.*, ***10***, 103 (1975).

[27] B. Bhattacharjee, S. Paul and R. Paul, *Mol. Phys.*, ***44***, 1391 (1981).

[28] B. Adhikari and R. Paul, *Phase Trans.*, ***56***, 153 (1996).

[29] J. Stamatoff, P.E. Cladis, D. Guilon, M.C. Cross, T. Bilash and P. Finn, *Physical Review Letters*, ***44 (23)***, 1509 (1980).